



## Oxic urban rivers as a potential source of atmospheric methane<sup>☆</sup>

Feng Zhao<sup>a,b</sup>, Yongqiang Zhou<sup>a</sup>, Hai Xu<sup>a,\*</sup>, Guangwei Zhu<sup>a</sup>, Xu Zhan<sup>b</sup>, Wei Zou<sup>a</sup>, Mengyuan Zhu<sup>a</sup>, Lijuan Kang<sup>a</sup>, Xingchen Zhao<sup>a</sup>

<sup>a</sup> State Key Laboratory of Lake and Environment, Nanjing Institute of Geography and Limnology, Chinese Academy of Sciences, Nanjing, 210008, PR China

<sup>b</sup> School of Environmental and Civil Engineering, Jiangnan University, Wuxi, 214122, PR China

### ARTICLE INFO

#### Keywords:

Methane (CH<sub>4</sub>)  
Urban river  
Algal blooms  
Human activities  
Xin'an river

### ABSTRACT

Urban rivers play a vital role in global methane (CH<sub>4</sub>) emissions. Previous studies have mainly focused on CH<sub>4</sub> concentrations in urban rivers with a large amount of organic sediment. However, to date, the CH<sub>4</sub> concentration in gravel-bed urban rivers with very little organic sediment has not been well documented. Here, we collected water samples from an oxic urban river (Xin'an River, China; annual mean dissolved oxygen concentration was  $9.91 \pm 1.99 \text{ mg L}^{-1}$ ) with a stony riverbed containing very little organic sediment. Dissolved CH<sub>4</sub> concentrations were measured using a membrane inlet mass spectrometer to investigate whether such rivers potentially act as an important source of atmospheric CH<sub>4</sub> and the corresponding potential drivers. The results showed that CH<sub>4</sub> was supersaturated at all sampling sites in the five sampling months. The mean CH<sub>4</sub> saturation ratio (ratio of river dissolved CH<sub>4</sub> concentration to the corresponding CH<sub>4</sub> concentration that is in equilibrium with the atmosphere) across all sampling sites in the five sampling months was  $204 \pm 257$ , suggesting that the Xin'an River had a large CH<sub>4</sub> emission potential. The CH<sub>4</sub> concentration was significantly higher in the downstream river than in the upstream river ( $p < 0.05$ ), which suggested that human activities along the river greatly impacted the CH<sub>4</sub> level. Statistical analyses and incubation experiments indicated that algae can produce CH<sub>4</sub> under oxic conditions, which may contribute to the significantly higher CH<sub>4</sub> concentration in August 2020 ( $p < 0.001$ ) when a severe algal bloom occurred. Furthermore, other factors, such as heavy rainfall events, dissolved organic carbon concentration, and water temperature, may also be vital factors affecting CH<sub>4</sub> concentration. Our study enhances the understanding of dissolved CH<sub>4</sub> dynamics in oxic urban rivers with very little organic sediment and further proposes feasible measures to control the CH<sub>4</sub> concentration in urban rivers.

### 1. Introduction

Methane (CH<sub>4</sub>) is an important greenhouse gas that contributes greatly to global warming (Montzka et al., 2011; Wang et al., 2020b). Despite its low concentration in the atmosphere compared with that of carbon dioxide (CO<sub>2</sub>), its warming effect is more than 28 times that of CO<sub>2</sub> (IPCC, 2013). Inland freshwater bodies (such as rivers, lakes, and reservoirs) are hotspots of global CH<sub>4</sub> emissions (Bastviken et al., 2011; Deemer et al., 2016; Stanley et al., 2016). It was reported that global CH<sub>4</sub> emissions from inland freshwater bodies reached 103.3 Tg CH<sub>4</sub> yr<sup>-1</sup>, and CH<sub>4</sub> emissions from rivers reached 1.5 Tg CH<sub>4</sub> yr<sup>-1</sup> based on measurements from regional-scale rivers (Bastviken et al., 2011). Among all rivers, urban rivers are considered relatively important sources of CH<sub>4</sub> emissions (Ortega et al., 2019; Li et al., 2020; Wang et al.,

2020a). According to a recent study conducted by Zhang et al. (2021b), the average CH<sub>4</sub> diffusive flux from urban rivers in the Chaohu Lake Basin of China was  $7 \text{ mmol CH}_4 \text{ m}^{-2} \text{ d}^{-1}$ , which was 7 times higher than that from nonurban rivers in that region. Similarly, high CH<sub>4</sub> ebullition was also observed from urban rivers (Wang et al., 2021). The greatest difference between river water and lake (or reservoir and ocean) water is that river water has a shorter water residence time. At the same time, urban rivers received a high level of pollutants (e.g., nutrients, organic matter, and CH<sub>4</sub>) due to intense human activities (Alshboul et al., 2016; Yin et al., 2021) and may become hotspots for CH<sub>4</sub> emission. Therefore, investigating the CH<sub>4</sub> dynamics in urban rivers can help us further understand its contribution to the CH<sub>4</sub> level in downstream waters and the global CH<sub>4</sub> budget.

Traditionally, CH<sub>4</sub> was considered to be primarily produced through

<sup>☆</sup> This paper has been recommended for acceptance by Pavlos Kassomenos.

\* Corresponding author. Nanjing Institute of Geography and Limnology, Chinese Academy of Sciences, 73 East Beijing Road, Nanjing, 210008, PR China.

E-mail address: [hxu@niglas.ac.cn](mailto:hxu@niglas.ac.cn) (H. Xu).

anaerobic fermentation of acetate driven by methanogens under strictly anoxic conditions (Zamanpour et al., 2020). However, CH<sub>4</sub> oversaturation has been observed in some oxic water columns (Karl et al., 2008; Damm et al., 2010; Tang et al., 2016), which seems to contradict the traditional concept. Traditional explanations for this paradox include transport from nearby anoxic sediment or shorelines (Hofmann et al., 2010) and production within microanoxic areas such as detritus (de Angelis and Lee, 1994). However, an increasing number of studies have found that CH<sub>4</sub> can also be produced under oxic conditions. Different from the prevailing paradigm that methanogens are strict anaerobes, some methanogens have been reported to be remarkably tolerant to oxygen (Angel et al., 2011), and some microorganisms may produce CH<sub>4</sub> through a different pathway that does not require oxygen-sensitive enzymes, which may be potential explanations for CH<sub>4</sub> oversaturation in fully aerobic waters (Tang et al., 2016). Furthermore, numerous studies have revealed that the CH<sub>4</sub> concentration was positively correlated with the Chl<sub>a</sub> concentration in oxic waters, which indicated that algae may play a role in the CH<sub>4</sub> paradox. CH<sub>4</sub> production driven by cyanobacteria has been attributed to the demethylation of methyl phosphonates (White et al., 2010). Recently, several studies demonstrated that algae can produce CH<sub>4</sub> by converting bicarbonate to CH<sub>4</sub> through photosynthesis under oxic conditions (Bižić et al., 2020; Günthel et al., 2020). In addition, some genera of cyanobacteria, such as *Anabaena*, have the ability to fix nitrogen, along with the production of CH<sub>4</sub>. For example, Conrad and Seiler (1980) observed high CH<sub>4</sub> concentrations during a nitrogen-fixing algal bloom in 2010. Zheng et al. (2018) reported that CH<sub>4</sub> could be produced by nitrogenase during nitrogen fixation. One possible mechanism for this is that nitrogen fixation induced by cyanobacteria can provide hydrogen for methanogens to produce CH<sub>4</sub> (Berg et al., 2014; Tang et al., 2014). Current studies have mainly focused on oxic CH<sub>4</sub> production in deep lakes and reservoirs and have pointed out that oxic CH<sub>4</sub> production made a large contribution to total CH<sub>4</sub> emissions from these waters (Donis et al., 2017; Günthel et al., 2019). However, to date, CH<sub>4</sub> oversaturation in gravel-bed urban rivers with very little organic sediment and its relationship with algae remain unclear.

Due to human activities or landforms, the riverbeds of some rivers

are stony and often covered with inorganic materials (e.g., gravels, coarse pebbles, and large stones) rather than organic sediment (Fig. 1d). It seems that the CH<sub>4</sub> concentrations in the water column in such rivers may be low since organic sediment is considered a hotspot for CH<sub>4</sub> production and is an important source of water column CH<sub>4</sub> (Conrad et al., 2009; Mach et al., 2015; Emilson et al., 2018). However, urban rivers are often polluted due to intense human activities. The pollution may cause algal blooms, which may have a potential impact on CH<sub>4</sub> concentration. Additionally, wastewater from municipal wastewater treatment plants (WWTPs) may also contain a large amount of dissolved CH<sub>4</sub> (Wang et al., 2011; Alshboul et al., 2016), which may be an additional source of CH<sub>4</sub> due to discharging the treated wastewater into the rivers (Alshboul et al., 2016). Thus, we speculate that the CH<sub>4</sub> concentration in these rivers may be underestimated. However, to the best of our knowledge, no study has focused on CH<sub>4</sub> concentration and its potential drivers in oxic urban rivers with very little organic sediment.

We hypothesized that oxic urban rivers with very little organic sediment could be a potential source of atmospheric CH<sub>4</sub> and that human activities and algal blooms could potentially affect CH<sub>4</sub> concentration in these rivers. Therefore, we chose an oxic urban river with a low amount of organic sediment as our study area. Five-month field observations and incubation experiments were conducted. The purposes of this study were (1) to measure the CH<sub>4</sub> concentrations to investigate whether oxic urban rivers with a low amount of organic sediment can act as a potential source of atmospheric CH<sub>4</sub>; (2) to explore potential factors affecting CH<sub>4</sub> concentrations in these rivers; and (3) to provide suggestions for managing CH<sub>4</sub> concentrations in these rivers.

## 2. Materials and methods

### 2.1. Study area

This study was conducted in the Xin'an River in Huangshan city, Anhui Province, China (Fig. 1a). The Xin'an River is located in the northern subtropics. The annual average temperature in this area is approximately 15 °C. The average temperatures range from 1 to 4 °C and 27–29 °C in January and July, respectively. The water originates from

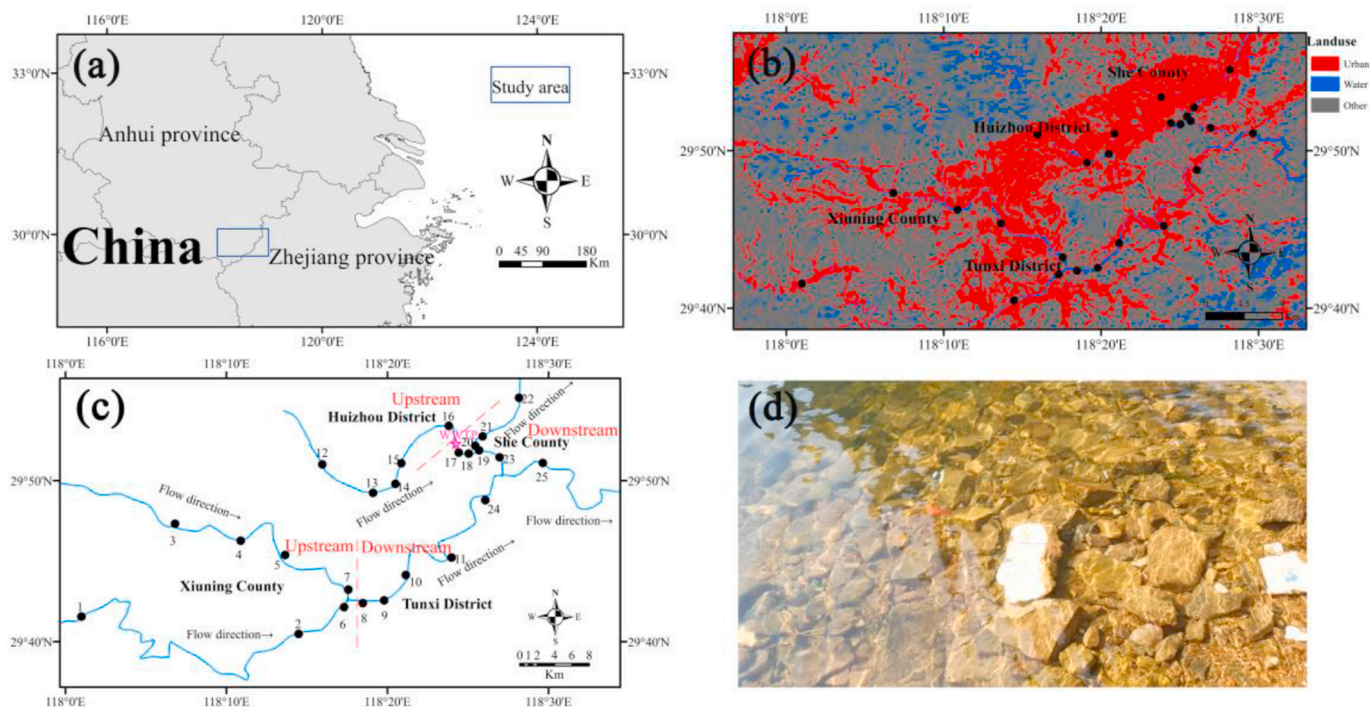


Fig. 1. (a) The study area, (b) land use in the sampling area, (c) specific sampling sites, and (d) sediment of the river.

Liugujian at the junction of Anhui Province and Jiangxi Province. The mainstream of Xin'an River in Anhui Province is 242.3 km long and covers an area of 6500 km<sup>2</sup>, accounting for 11.9% of the area of the Qiantang River Basin. Xin'an River contains two large tributaries (Tributary 1 and Tributary 2, Fig. 1c). Tributary 1 contains two smaller tributaries (Hengjiang and Jianjiang), which converge in Tunxi District. Xiuning County (sites 1–7) is located upstream of Tributary 1, while Tunxi District (sites 8–11, 24) is located downstream of Tributary 1. Tributary 2 includes two urban areas, Huizhou District and She County. Huizhou District (sites 12–16) is the upstream area, and She County (sites 17–23, 25) is the downstream area. Sites 17–20 are the nearest four sites downstream of the WWTP (within 3 km, Fig. 1c). The riverbed of the Xin'an River is mainly covered with inorganic sediment (e.g., gravels, coarse pebbles, and large stones) rather than organic sediment (Fig. 1d).

We selected 25 sites from the upstream Xin'an River to the confluence of Xin'an Reservoir. These sampling sites were located in four areas, including Xiuning County, Tunxi District, Huizhou District, and She County, which are four urban areas of Huangshan city (Fig. 1b). Water samples were collected in July 2020 (rainy month), August 2020 (summer), October 2020 (autumn), January 2021 (winter), and April 2021 (spring). The spatial distribution of the sampling sites is shown in Fig. 1c.

## 2.2. Sample collection

A 5-L water sampler (Uwitec, Austria) was used to collect 5 L of surface water from bridges, and a peristaltic pump (Jihpump, China) connected with a gas-tight rubber tube (internal diameter: 3 mm, Yingtong, China) was used to transfer the bubble-free water to a 12 mL vial (Labco Exetainer, UK). One end of the rubber tube was placed 10 cm below the surface water in the water sampler because the direct collection of surface water might cause bubbles and affect the subsequent measurement. The other end was placed in the vial. The vial was screwed tightly with no headspace after being filled with water. Two quantitative syringes (Cofee, China) were used to add 0.1 mL of saturated ZnCl<sub>2</sub> solution for microbial inactivation. Three duplicate samples were prepared. These samples were collected to measure the N<sub>2</sub>:Ar ratio and CH<sub>4</sub> concentration using a membrane inlet mass spectrometer (MIMS, Bay Instrument, USA). A 2 L water sample was transferred to a clean plastic bottle and then placed into a cooling box for subsequent measurement of physical and chemical properties. Lugol iodine solution was added to a 1 L water sample to identify the algal community structure.

## 2.3. Measurement of key water quality parameters

Water temperature (WT), dissolved oxygen (DO), and fluorescent dissolved organic matter (fDOM) were measured by a multisensor sonde (YSI 6600 V2, USA). A 100 mL unfiltered water sample was used to determine the concentrations of total nitrogen (TN) and total phosphorus (TP). A 500 mL water sample was filtered through 0.70- $\mu$ m membrane filters (Whatman GF/F, UK) for subsequent determination of the concentrations of chlorophyll *a* (Chl*a*) and dissolved organic carbon (DOC). The measurements of nutrients and Chl*a* concentrations were done according to standard methods (APHA, 2012). The DOC concentrations were measured using a Shimadzu TOC-L analyzer. The samples for identifying the algal community structure and algal concentration were treated with a Lugol iodine solution (1%, V/V) and allowed to settle for 48 h. The cell density was then directly measured in a 0.1 mL counting chamber (Hengke, China), and an Olympus BX53 microscope was used at a magnification of 400 $\times$ . The method for identifying algae was derived from Hu and Wei (2007).

## 2.4. Method for quantifying the nitrogen fixation capacity and CH<sub>4</sub> concentration

The method for quantifying the nitrogen fixation capacity in this study was the N<sub>2</sub>:Ar method, a relatively new method that has been widely used in aquatic environments (Schmale et al., 2019; Loeks-Johnson and Cotner, 2020; Zhao et al., 2022). The analytical instrument was MIMS, which has been used to measure concentrations of dissolved N<sub>2</sub>, Ar, and O<sub>2</sub> in natural water samples for decades (Kana et al., 1994). More details about this method can be obtained from previous studies (Schmale et al., 2019; Loeks-Johnson and Cotner, 2020). MIMS was also used to measure the dissolved CH<sub>4</sub> concentration instead of the traditional method (headspace combined with gas chromatography) since the MIMS method has a great advantage in CH<sub>4</sub> determination compared with the traditional method. More details regarding the MIMS method for measuring CH<sub>4</sub> concentration and its advantages can be found in the reference (Zhao et al., 2021).

## 2.5. Calculations of CH<sub>4</sub>, O<sub>2</sub>, and N<sub>2</sub>: Ar saturation ratio

Water flow velocity, the slope of the river, wind speed, and WT are important factors that control CH<sub>4</sub> diffusion from rivers (Borges et al., 2018; Wang et al., 2020a). CH<sub>4</sub> diffusion can be obtained from direct measurement using floating chambers or calculated based on models using the factors mentioned above (Clough et al., 2007; Zhang et al., 2021b). Because we did not measure the water flow velocity and the slope of the river, we only calculated the CH<sub>4</sub> saturation ratio. Although the CH<sub>4</sub> saturation ratio cannot directly reveal the CH<sub>4</sub> emissions from rivers to the atmosphere, it can represent the CH<sub>4</sub> emission potential.

The CH<sub>4</sub> saturation ratio was calculated using the following equation: where C<sub>m</sub> represents the measured CH<sub>4</sub> concentration ( $\mu$ mol L<sup>-1</sup>) using MIMS and C<sub>eq</sub> ( $\mu$ mol L<sup>-1</sup>) is the equilibrium CH<sub>4</sub> concentration under the corresponding temperature, which was calculated through WT, atmospheric pressure, and volume ratio of CH<sub>4</sub> to the air of the ambient air (Xiao et al., 2017). A CH<sub>4</sub> saturation ratio >1 indicates that CH<sub>4</sub> is supersaturated in the water, while a CH<sub>4</sub> saturation ratio <1 represents CH<sub>4</sub> undersaturation.

The calculations of DO and N<sub>2</sub>:Ar saturation ratios were the same as that of CH<sub>4</sub>.

## 2.6. Incubation experiment

An incubation experiment was conducted to test the effect of algae, sediment, and organic soils from the riparian zone on CH<sub>4</sub> concentrations in oxic water in the Xin'an River in September 2021. Five treatments were performed. Treatment 1 (T1): 1 L of river water was collected and filtered using a 64- $\mu$ m filter screen (Hengke, China) to remove the algae. Then, the filtered water was transferred to a gas-tight and transparent incubation core. Treatment 2 (T2): 1 L of river water (Chl*a* concentration 112.1  $\mu$ g L<sup>-1</sup>) was collected into a gas-tight and transparent incubation core. The core was sealed without headspace using a gas-tight tip. Treatment 3 (T3): Based on T2, algae collected from the river were added to the core and ensured that the final Chl*a* concentration was  $\sim$ 200  $\mu$ g L<sup>-1</sup>. Treatment 4 (T4): Based on T2, organic solids were collected from the nearby riparian zone and were added to the core (volume ratio (organic solids: water column = 1: 5)). Treatment 5 (T5): Based on T2, sediments (mainly composed of gravels and pebbles) were collected from the river and were added to the core (volume ratio (sediments: water column = 1: 5)). Three replicates were conducted for each of the five treatments. The incubation cores were placed into the river to ensure that the growth of algae was not limited by light. Furthermore, algae can produce O<sub>2</sub> through photosynthesis under light thereby facilitating oxic conditions in the water. The incubation experiment lasted for 7 days. Water (20 mL) was collected each day to measure the concentrations of dissolved CH<sub>4</sub> and DO using MIMS. The 20-mL water was replaced by 20-mL distilled water using two 30-mL gas-tight



syringes (Cofee, China). On the last day, the overlying water was pumped using a peristaltic pump, and the water was prepared to measure the concentrations of TN, TP, Chla, and DOC. More details regarding the incubation experiment can be found in the supporting information.

## 2.7. Data analyses

IBM SPSS 19.0 was used to analyse the spatial and temporal differences in variables (e.g., CH<sub>4</sub> concentration and key water quality parameters). If the data met the normality, independence, and homogeneity of variance criteria, one-way ANOVA (analysis of variance) was used. If the data met the normality and independence criteria but not the homogeneity of variance criteria, Welch corrected analysis of variance was used. If the preconditions of the parametric test were not met, the nonparametric Kruskal–Wallis test was used. The selection of the multiple comparison method adopts the LSD (least significant difference) test according to whether the data meet the homogeneity of variance. If the *p* value is less than 0.05, it indicates that there is a significant spatial (or temporal) difference in variables. The box plot was used to statistically show the differences in dissolved CH<sub>4</sub> concentrations between the upstream river and downstream river, as well as the differences among five different sampling months. All correlations were completed using Pearson correlation analysis with *p* < 0.05 indicating a significant correlation between two variables. Logarithmic treatment was performed if necessary. The analytical software was IBM SPSS 19.0. Figures were completed using Origin 9.5 and ArcGIS 10.4.1.

## 3. Results

### 3.1. Characteristics of key physical and chemical variables

The average WT was  $27.1 \pm 1.49$  °C,  $32.8 \pm 1.04$  °C,  $19.4 \pm 0.81$  °C,  $8.67 \pm 1.60$  °C and  $19.9 \pm 1.36$  °C in July 2020, August 2020, October 2020, January 2021, and April 2021, respectively (Table 1). The DO concentration was high at most sampling sites in the five sampling months, ranging from  $6.38$  to  $16.0$  mg L<sup>-1</sup> (Table S1), with a mean concentration of  $9.91 \pm 1.99$  mg L<sup>-1</sup>. A high TN concentration ( $1.63 \pm 0.48$  mg L<sup>-1</sup>) was observed in July 2020, but it decreased significantly in August 2020 (*p* < 0.001), with an average value of  $1.07 \pm 0.52$  mg L<sup>-1</sup> (Table 1). The mean TN concentration increased noticeably in October 2020 and January 2021, particularly in January 2021. The monthly variations in TP concentrations were very different compared with those of TN. The lowest TP concentration was observed in October 2020, with

**Table 1**  
Key variables of the water samples in the five months.

	July 2020	August 2020	October 2020	January 2021	April 2021
	Mean ± SD	Mean ± SD	Mean ± SD	Mean ± SD	Mean ± SD
WT (°C)	27.1 ± 1.49	32.8 ± 1.04	19.4 ± 0.81	8.67 ± 1.60	19.9 ± 1.36
DO (mg L <sup>-1</sup> )	8.11 ± 0.10	9.48 ± 2.20	10.1 ± 1.11	11.5 ± 2.03	10.4 ± 1.58
TN (mg L <sup>-1</sup> )	1.63 ± 0.48	1.07 ± 0.52	1.39 ± 0.62	2.10 ± 0.98	1.54 ± 0.42
TP (µg L <sup>-1</sup> )	92.8 ± 50.0	78.7 ± 4.64	46.7 ± 28.1	79.0 ± 69.6	67.4 ± 30.5
N:P ratio	19.3 ± 3.86	14.5 ± 3.17	33.6 ± 11.6	35.1 ± 15.2	25.0 ± 6.79
DOC (mg L <sup>-1</sup> )	1.53 ± 0.52	2.05 ± 0.51	1.39 ± 0.53	1.34 ± 0.57	1.37 ± 0.35
Chla (µg L <sup>-1</sup> )	3.69 ± 4.36	22.5 ± 24.8	3.13 ± 3.31	2.36 ± 1.35	8.55 ± 5.25
CH <sub>4</sub> (µmol L <sup>-1</sup> )	0.47 ± 0.31	1.19 ± 1.02	0.42 ± 0.46	0.33 ± 0.27	0.51 ± 0.51

a mean value of  $46.7 \pm 28.1$  µg L<sup>-1</sup>, while the highest value appeared in July 2020 (Table 1). The N:P ratio was low in summer, with a mean value of  $14.5 \pm 3.17$ , but it was high in other seasons, especially in winter, with a mean value reaching  $35.1 \pm 15.2$ . The Chla concentrations were high in August 2020, ranging from  $1.26$  to  $95.5$  µg L<sup>-1</sup>, but were low in the other four months (Table S1). The organic carbon concentrations were very low in Xin'an River, and the average concentrations of DOC in July 2020, August 2020, October 2020, January 2021, and April 2021 were  $1.53 \pm 0.52$  mg L<sup>-1</sup>,  $2.05 \pm 0.51$  mg L<sup>-1</sup>,  $1.39 \pm 0.53$  mg L<sup>-1</sup>,  $1.34 \pm 0.57$  mg L<sup>-1</sup>, and  $1.37 \pm 0.35$  mg L<sup>-1</sup>, respectively (Table 1). On a spatial scale, TN and TP concentrations across the sampling sites also showed large variation. Generally, the annual mean concentrations of TN, TP, and Chla were significantly higher in the downstream river than those in the upstream river (*p* < 0.001 for TN and TP and *p* = 0.029 for Chla).

### 3.2. Gas saturation ratio

The CH<sub>4</sub> supersaturation ratio appeared highest in August 2020, reaching  $479 \pm 415$ , followed by July 2020 with  $174 \pm 115$ . High mean values were also observed in October 2020 and April 2021, with values of  $136 \pm 150$  and  $167 \pm 166$ , respectively. The lowest values appeared in January 2021, with a mean value of  $81.1 \pm 66.7$  (Fig. 2a). DO supersaturation was observed in July 2020, August 2020, October 2020, and April 2021, which was  $1.02 \pm 0.13$ ,  $1.32 \pm 0.32$ ,  $1.10 \pm 0.12$ , and  $1.14 \pm 0.18$ , respectively, while it was unsaturated in January 2021, which was  $0.98 \pm 0.16$  (Fig. 2b). In August 2020, we observed that N<sub>2</sub> was unsaturated with a mean N<sub>2</sub>:Ar saturation ratio of  $0.97 \pm 0.008$  and was significantly lower than that in July 2020, October 2020, January 2021, and April 2021 (*p* < 0.001), with a mean N<sub>2</sub>:Ar saturation ratio of  $1.01 \pm 0.002$ ,  $0.999 \pm 0.007$ ,  $1.01 \pm 0.005$ , and  $1.00 \pm 0.007$ , respectively (Fig. 2c).

### 3.3. Spatial and temporal variations in CH<sub>4</sub> concentrations

On a temporal scale, the CH<sub>4</sub> concentration was significantly higher in August 2020 than in the other four months (*p* < 0.05, Table S2 and Fig. 3a), with a mean value of  $1.19 \pm 1.02$  µmol L<sup>-1</sup>. However, there was no significant temporal difference in CH<sub>4</sub> concentration among the other four months (*p* > 0.05, Table S2 and Fig. 3a). The CH<sub>4</sub> concentration in October 2020 was slightly lower than that in July 2020, with an average of  $0.42 \pm 0.46$  µmol L<sup>-1</sup>. In January 2021, the mean dissolved CH<sub>4</sub> concentration was  $0.33 \pm 0.27$  µmol L<sup>-1</sup>, which was the lowest among the five sampling months (Fig. 3a). Similarly, the distribution of dissolved CH<sub>4</sub> concentration also showed a large difference on a spatial scale. Generally, the dissolved CH<sub>4</sub> concentration was low in the upstream river, but it was significantly higher in the downstream river, especially in She County (*p* < 0.05, Table S2 and Fig. 3b). As shown in Fig. 3b, the mean CH<sub>4</sub> concentration of the five sampling months was  $0.26 \pm 0.28$  µmol L<sup>-1</sup> in upstream Xiuning County, but it was significantly higher in downstream Tunxi District (*p* < 0.05,  $0.66 \pm 0.83$  µmol L<sup>-1</sup>). Similarly, a low CH<sub>4</sub> concentration was found in upstream Huizhou District ( $0.49 \pm 0.41$  µmol L<sup>-1</sup>), but it was significantly higher in downstream She County (*p* < 0.05,  $0.88 \pm 0.73$  µmol L<sup>-1</sup>). A significant difference in dissolved CH<sub>4</sub> concentration was observed between Tributary 1 and Tributary 2 (*p* < 0.001, Table S2 and Fig. 3c), with mean dissolved CH<sub>4</sub> concentrations of  $0.43 \pm 0.61$  µmol L<sup>-1</sup> and  $0.72 \pm 0.65$  µmol L<sup>-1</sup> for Tributary 1 and Tributary 2, respectively. Furthermore, the CH<sub>4</sub> concentrations were much higher at sites near a large WWTP ( $1.25 \pm 0.83$  µmol L<sup>-1</sup>) than at the other sites ( $0.45 \pm 0.52$  µmol L<sup>-1</sup>) in the five sampling months (*p* < 0.001, Table S2 and Fig. 3d).

### 3.4. Pearson correlation analyses

Fig. 4 shows the results of the Pearson correlation analysis. DOC and FDOM were positively correlated with the CH<sub>4</sub> saturation ratio (*p* <

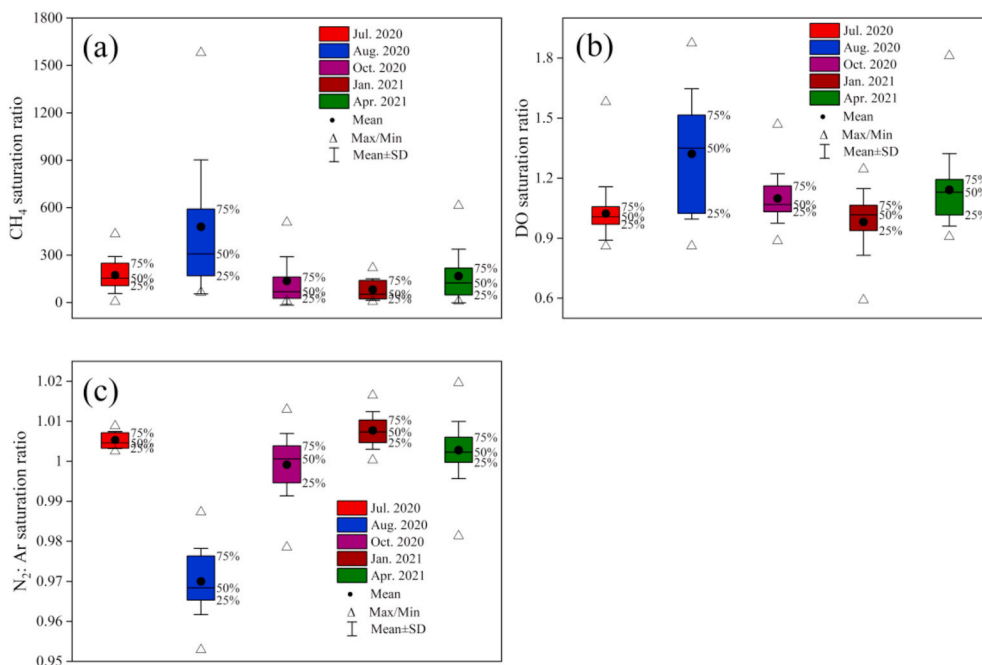


Fig. 2. A, b, and c show the box plots of the CH<sub>4</sub> saturation ratio, DO saturation ratio, and N<sub>2</sub>:Ar saturation ratio in the five sampling months, respectively.

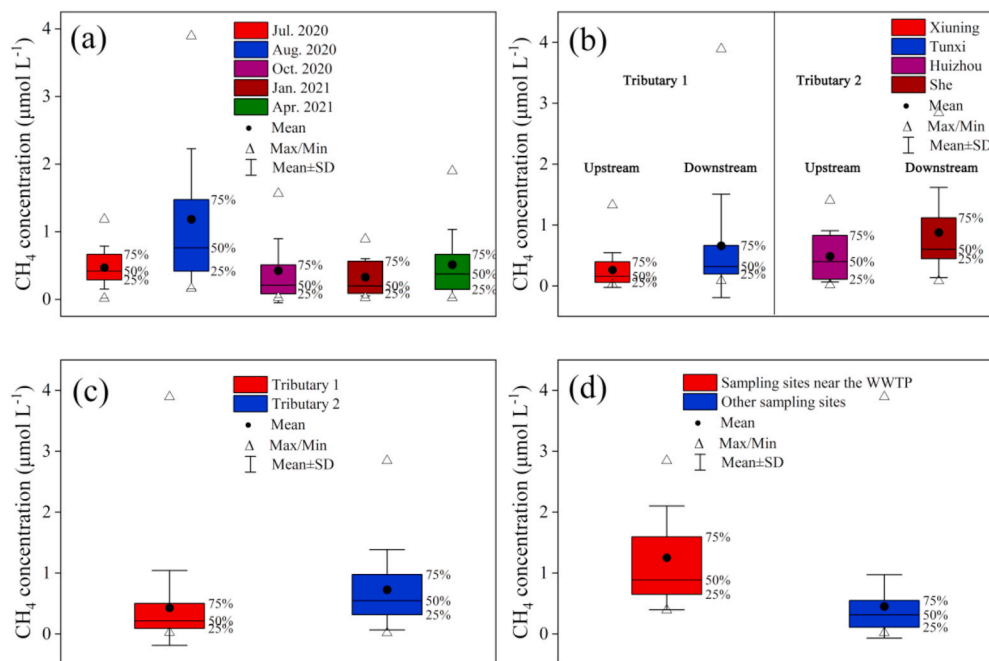


Fig. 3. (a) Temporal changes in dissolved CH<sub>4</sub> concentrations; (b) spatial differences in dissolved CH<sub>4</sub> concentrations between the upstream river and downstream river in the two tributaries (For Tributary 1, Xiuning County is the upstream river and Tunxi District is the downstream river; For Tributary 2, Huizhou District is the upstream river and She County is the downstream river); (c) spatial differences in dissolved CH<sub>4</sub> concentrations between Tributary 1 and Tributary 2; and (d) spatial differences in dissolved CH<sub>4</sub> concentrations between four nearest sites (site 17–20) at the downstream of the WWTP and other sites.

0.001). A positive correlation was found between WT and CH<sub>4</sub> saturation ratio ( $p < 0.001$ ). A significant positive correlation appeared between the CH<sub>4</sub> saturation ratio and TP concentration ( $p < 0.001$ ). No significant correlation was observed between CH<sub>4</sub> saturation ratio with TN concentration ( $p > 0.05$ ). Interestingly, the CH<sub>4</sub> saturation ratio was positively correlated with the N:P ratios ( $p < 0.001$ ). A significant positive correlation was also observed between the CH<sub>4</sub> saturation ratio and Chl<sub>a</sub> concentration ( $p < 0.001$ ). We observed that the concentration of DO was positively correlated with the CH<sub>4</sub> saturation ratio ( $p < 0.001$ ). The CH<sub>4</sub> saturation ratio also exhibited a significant correlation with the N<sub>2</sub> saturation ratio ( $p < 0.001$ ); however, this correlation was negative, which was different from that of the DO saturation ratio.

### 3.5. Algal communities in Xin'an River

On a temporal scale, Bacillariophyta was the dominant phylum in July 2020, October 2020, January 2021, and April 2021, accounting for 47.29%, 47.77%, 85.32%, and 79.39%, respectively (Fig. 5a). In contrast, the proportion of Bacillariophyta was low in August 2020, accounting for only 10.03%. The contribution of Cyanophyta was high in July 2020, August 2020, and October 2020, which accounted for 38.92%, 40.44%, and 29.07%, respectively. A high Chlorophyta concentration was observed in August 2020, but it was very low in the other four months. The concentrations of the other three phyla, Pyrrophyta, Cryptophyta, and Euglenophyta, were very low in all sampling months

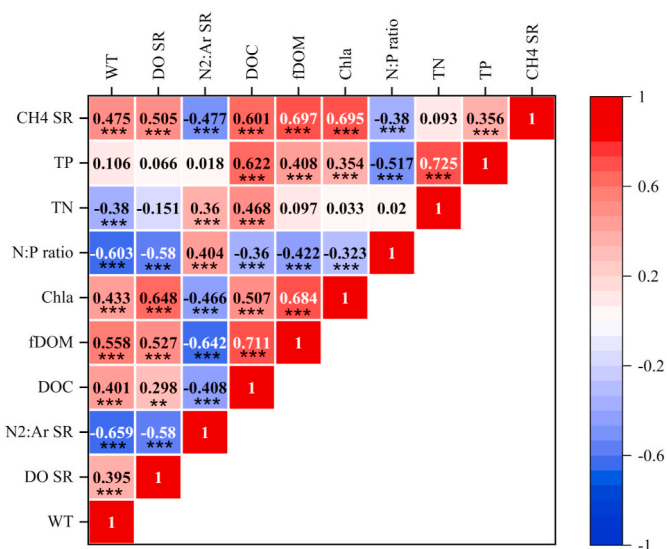


Fig. 4. Pearson correlation analysis of the environmental variables. SR indicates saturation ratio. \*\* and \*\*\* indicate  $p < 0.01$  and  $p < 0.001$ , respectively.

(Fig. 5a). A high concentration of *Anabaena* was found in August 2020, but the *Anabaena* concentration was low in July 2020 and January 2021. No *Anabaena* was observed in October 2020 or April 2021 (Fig. 5b).

On a spatial scale, Bacillariophyta was the dominant phylum in the Xin'an River in July 2020, but the contribution of Cyanophyta to the total algal community was high in some areas (e.g., Tunxi District, Fig. S1). In contrast, the Xin'an River was dominated by Cyanophyta and Chlorophyta, and the proportion of Cyanophyta to the total community in the downstream river was much higher than that in the upstream river in August 2020. High proportions of Cyanophyta to the total community were also found in She County, but Chlorophyta was replaced by Bacillariophyta. The Cyanophyta concentration, as well as the proportion of Cyanophyta to the total community, was very low at all sampling sites in January 2021 and April 2021, and Bacillariophyta had a great advantage in community competition. High *Anabaena* concentrations were observed in the downstream river (Tunxi District and She County). However, very low *Anabaena* concentrations appeared in the other three months, and most sampling sites had no *Anabaena* (Fig. S2).

### 3.6. Incubation experiment

Fig. 6a shows the CH<sub>4</sub> concentrations in the five treatments during incubation experiments. The dissolved CH<sub>4</sub> concentration in the incubation core was almost 0 before incubation. No evident CH<sub>4</sub> accumulation was observed in T1, while obvious CH<sub>4</sub> production was found in the other five treatments. After a 7-day incubation, the final CH<sub>4</sub>

concentrations were  $0.006 \pm 0.006 \mu\text{mol L}^{-1}$ ,  $0.08 \pm 0.01 \mu\text{mol L}^{-1}$ ,  $0.12 \pm 0.01 \mu\text{mol L}^{-1}$ ,  $0.26 \pm 0.02 \mu\text{mol L}^{-1}$ , and  $0.08 \pm 0.03 \mu\text{mol L}^{-1}$  in T1, T2, T3, T4, and T5, respectively. Fig. 6b shows the DO concentrations during incubation experiments. The DO concentration decreased from  $8.93 \pm 0.09 \text{ mg L}^{-1}$  to  $7.50 \pm 0.44 \text{ mg L}^{-1}$  in T1. In contrast, DO concentrations increased sharply in the other four treatments, with final concentrations of  $15.3 \pm 1.00 \text{ mg L}^{-1}$ ,  $16.4 \pm 0.82 \text{ mg L}^{-1}$ ,  $16.1 \pm 0.80 \text{ mg L}^{-1}$ , and  $15.4 \pm 0.56 \text{ mg L}^{-1}$  for T2, T3, T4, and T5, respectively. The concentrations of TN and TP were highest in T4. High Chla concentration was observed in T3.

## 4. Discussion

### 4.1. Potential factors affecting CH<sub>4</sub> concentrations in the Xin'an River

#### 4.1.1. Exogenous input

Organic sediment CH<sub>4</sub> production has been considered a crucial source of dissolved CH<sub>4</sub> in water columns according to previous studies (Conrad et al., 2009; Mach et al., 2015; Emilson et al., 2018). In this study, a stony riverbed covered with inorganic sediment (e.g., gravels, coarse pebbles, and large stones) was found along the entire Xin'an River (Fig. 1d). A previous study indicated that a microanoxic environment may form in deep sediment or within small inorganic particles and that this anoxic environment may be beneficial for anoxic CH<sub>4</sub> production (Hlaváčová et al., 2005). However, although we observed an increase in CH<sub>4</sub> concentration when adding sediments collected from the riverbed during the incubation experiment, this increase was very low (T5, Fig. 6a), indicating that the dissolved CH<sub>4</sub> was possibly from other pathways, such as oxic CH<sub>4</sub> production or directly from human discharged wastewater. The CH<sub>4</sub> concentrations were remarkably higher in the downstream river than in the upstream river ( $p < 0.05$ , Fig. 3b, Table S2), suggesting that human activities along the river had a strong influence on the CH<sub>4</sub> level. Alshboul et al. (2016) reported that the CH<sub>4</sub> in wastewater from WWTPs may potentially increase the CH<sub>4</sub> level in river water, which is similar to our results. In our study, we observed that the CH<sub>4</sub> concentrations at the four sampling sites near a large WWTP were significantly higher than those at other sampling sites (Fig. 3d), suggesting that high CH<sub>4</sub> concentrations there may have been related to wastewater from the WWTP.

Previous studies have shown that riparian zones of the river may be hotspots for CH<sub>4</sub> emissions (Sun et al., 2013), and changes in hydrological conditions may affect CH<sub>4</sub> emissions in the water level fluctuation zone (Shi et al., 2021). Here, we collected organic soils from the riparian zone and conducted an incubation experiment under flooding conditions. The results showed that the presence of organic soils could significantly increase the CH<sub>4</sub> concentration in the water (T4, Fig. 6a). This may have been because the overlying water separated the soil from the atmosphere, and the DOC in the porewater may have been converted to CH<sub>4</sub> by methanogens under anoxic conditions, which could result in an increase in dissolved CH<sub>4</sub> concentration in the water column. This

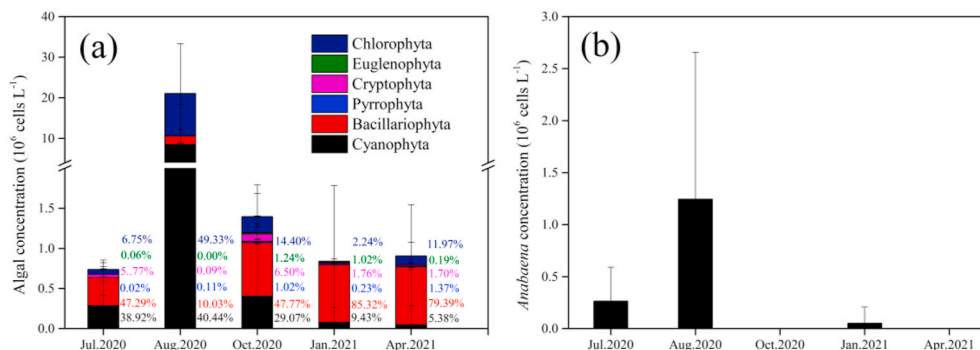
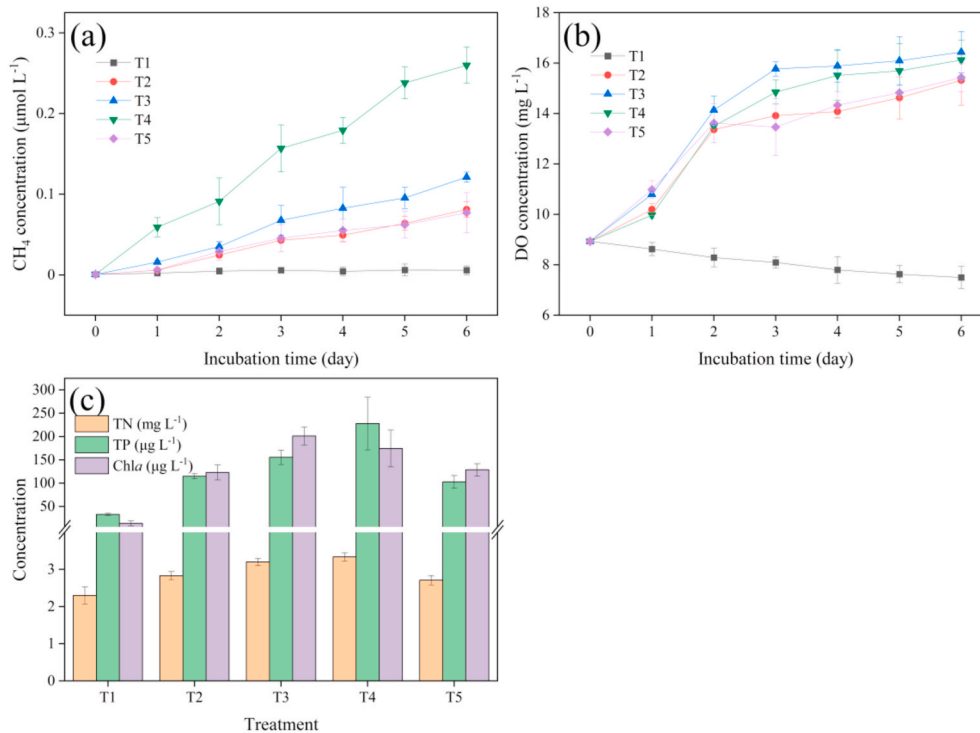


Fig. 5. (a) Algal communities over five months in the Xin'an River and (b) the concentration of *Anabaena*.



**Fig. 6.** Concentrations of dissolved CH<sub>4</sub> (a) and O<sub>2</sub> (b) in the incubation experiment. (c) Concentrations of TN, TP, and Chla in the water on the last day. Error bars represent standard deviations. T1: river water with no algae; T2: river water; T3: river water + algae; T4: river water + organic solids collected from the riparian zone; T5: river water + sediment.

experiment showed that when surface water flows through the riparian zone, it may produce CH<sub>4</sub> that is discharged into the river, thus affecting the CH<sub>4</sub> concentration in the river water. The water level fluctuation and the increase in surface runoff caused by rainfall may expand this contribution to the CH<sub>4</sub> level in the river. In addition, although there is very little organic sediment in the mainstream of the Xin'an River, there may be a large amount of organic sediment in some relatively small and quiet tributaries or bays. According to our incubation experiment, the CH<sub>4</sub> production capacity of organic soils was stronger than that of high-concentration algae (Fig. 6a). In this case, small and quiet bays or tributaries may be hotspots for CH<sub>4</sub> production, and the produced CH<sub>4</sub> may diffuse laterally into the mainstream. Additionally, the CH<sub>4</sub> in the groundwater was reported to be very high (Taylor et al., 2021), which could be a potential source of river CH<sub>4</sub>.

#### 4.1.2. Algae and nutrient concentration

We analysed the correlation between the CH<sub>4</sub> saturation ratio and environmental factors based on Pearson correlation analysis. The results showed that DOC and fDOM were positively correlated with CH<sub>4</sub> saturation ratio (Fig. 4). This is because organic carbon is the substrate for anoxic methanogenesis. This seems contrary to our conclusion that CH<sub>4</sub> can be produced in oxic water. In fact, having algal particles and microcolonies may create anoxia, which could provide a suitable environment for anoxic methanogenesis. It has been shown that cyanobacteria often host methanogenic archaea (Batista et al., 2019; Cook et al., 2019). Therefore, we observed high CH<sub>4</sub> concentrations and saturation ratios, along with high cyanobacterial density in August 2020 when algal blooms occurred due to high temperature (Figs. 2 and 5). Interestingly, we found a significant positive correlation between the CH<sub>4</sub> saturation ratio and DO saturation ratio ( $p < 0.001$ , Fig. 4), which was different from the results in other studies (Xiao et al., 2021; Zhang et al., 2021b). We attributed this paradox to photosynthesis induced by algae since we observed a significant positive correlation between Chla concentration and DO saturation ratio ( $p < 0.001$ , Fig. 4). Although algae-induced photosynthesis is not beneficial for anoxic

methanogenesis because it can produce O<sub>2</sub> that would poison methanogenic archaea, its ability to produce DOC can support anoxic methanogenesis. Consequently, methanogenic archaea may adhere to algae and utilize the DOC derived from discharged human wastewater and/or photosynthesis to produce CH<sub>4</sub>. Furthermore, an increasing number of studies have found that algae could convert bicarbonate to CH<sub>4</sub> under oxic conditions during photosynthesis (Günthel et al., 2020). A recent study also demonstrated that nitrogen-fixing cyanobacteria could produce CH<sub>4</sub> during nitrogen fixation (Zheng et al., 2018). In our study, we observed that the concentration of *Anabaena* (nitrogen-fixing cyanobacteria) was significantly higher in August 2020 than in the other four months ( $p < 0.01$ , Fig. 5b), and N<sub>2</sub> was unsaturated in this period (Fig. 2c), suggesting that nitrogen fixation could be another pathway to produce CH<sub>4</sub>. A possible mechanism pointed out by Tang et al. (2014) is that nitrogen fixation can produce hydrogen for CH<sub>4</sub> production. Previous studies have demonstrated that oxic CH<sub>4</sub> production can contribute greatly to the atmospheric CH<sub>4</sub> budget in deep lakes and reservoirs (Donis et al., 2017; Günthel et al., 2019). In our study, although we did not quantify the specific contribution of oxic CH<sub>4</sub> production to CH<sub>4</sub> concentration, we observed that the Chla concentration was positively correlated with the CH<sub>4</sub> saturation ratio (Fig. 4), suggesting that algae may also have an impact on CH<sub>4</sub> levels in rivers. Furthermore, the incubation experiment also indicated that algae can produce CH<sub>4</sub> under oxic conditions (T3, Fig. 5a). No evident CH<sub>4</sub> accumulation was observed when adding sediment collected from the riverbed (T5, Fig. 5a), indicating that the CH<sub>4</sub> in the water column in the Xin'an River was not produced mainly from sediment. However, the relative contribution of oxic CH<sub>4</sub> production induced by algae to the CH<sub>4</sub> concentration in the water column was much lower compared with the treatment that was added with organic solids (from the riparian zone) in the incubation experiment (T4, Fig. 5a), suggesting that the riparian zone may be a hotspot for CH<sub>4</sub> production under flooding, which is similar to the results in a recent study (Shi et al., 2021). These results indicated that oxic CH<sub>4</sub> production caused by algae may potentially increase the CH<sub>4</sub> concentration in gravel-bed rivers with very little



organic sediment, but its specific contribution is unknown and needs further study.

Numerous studies have revealed that CH<sub>4</sub> production and emissions are associated with the eutrophication of waters. A significant correlation between CH<sub>4</sub> concentration or emission rate and nutrient concentrations was found in these studies (Zhang et al., 2021a; Xiao et al., 2021). Similar results were also observed in our study (Fig. 4). However, we found that the correlation between the CH<sub>4</sub> saturation ratio and TP concentration was more significant than that between the CH<sub>4</sub> saturation ratio and TN. We attributed this to the high N:P ratios. As shown in Table 1, the N:P ratios were very high in July 2020, October 2020, January 2021, and April 2021 and were even higher than the Redfield value (N:P ratio = 16). Besides, significant correlations between Chl<sub>a</sub> concentration with TP concentration and N:P ratio were observed but no significant correlation was found between Chl<sub>a</sub> concentration and TN concentration, which suggested that the growth of algae was generally limited by phosphorus rather than nitrogen during these four months. As a result, the nutrient could indirectly affect methanogenesis by controlling primary productivity, such as inducing the growth of algae. Furthermore, the low N:P ratio could shift the algal community from nonnitrogen-fixing algae to nitrogen-fixing cyanobacteria (Smith, 1983), which may also have an impact on the CH<sub>4</sub> concentration.

#### 4.1.3. Rainfall events

The mean dissolved CH<sub>4</sub> concentration during the rainy month (July 2020) was significantly lower than that in August 2020 ( $p < 0.001$ , Fig. 3a) but relatively higher than those in the other three sampling months, which seems to contradict our conjecture that rainfall may lead to water level fluctuations, resulting in the lateral diffusion of CH<sub>4</sub> from the riparian zone to the river. Here, we discuss some potential reasons for this phenomenon. First, the very high precipitation during July 2020 (Fig. 7) may have diluted the CH<sub>4</sub> concentration in the river. Second, the disturbance caused by heavy rainfall may have aggravated CH<sub>4</sub> emissions (diffusion and ebullition) from the water to the atmosphere, resulting in a decline in the dissolved CH<sub>4</sub> concentration in the river. Third, the nutrient concentrations during the rainy period were generally higher than those during the post-rainy period (Table 1), but we observed that the Chl<sub>a</sub> concentrations were much lower than those in August 2020 ( $p < 0.001$ , Table 1). Heavy rainfall shifts the river to the flood period, resulting in a higher water velocity, while rapid flushing due to high water velocity is not conducive to the growth of cyanobacteria (Reynolds et al., 2006; Zou et al., 2020). As evidenced by the incubation experiment (Fig. 6), the presence of algae can significantly promote methanogenesis, which may be an important explanation for the lower CH<sub>4</sub> concentration in July 2020 compared with that in August 2020. Fourth, the increase of water discharge caused by heavy rainfall events may have reduced the river CH<sub>4</sub> level because the high water discharge can increase the CH<sub>4</sub> emission and reduce the CH<sub>4</sub> concentration according to a previous study (McGinnis et al., 2016). Fifth, we observed that the concentrations of DOC and FDOM during the rainy

period were lower than those in August 2020 (Table 1), which may have been an important reason for the low concentration of CH<sub>4</sub>. Last but not least, the low temperature caused by heavy rainfall (Fig. 7) could be another reason why the CH<sub>4</sub> concentrations were lower in July 2020 than in August 2020 since temperature is a vital factor that could affect CH<sub>4</sub> production (Yvon-Durocher et al., 2014).

#### 4.1.4. WT

In this study, we found that the concentration of CH<sub>4</sub> in August 2020 with high WT was significantly higher than that in January 2021 with low WT ( $p < 0.001$ , Table 1). The dissolved CH<sub>4</sub> concentration in August 2020 was 3.61 times higher than that in January 2021. A significant relationship was also observed between the WT and CH<sub>4</sub> saturation ratio (Fig. 4). These findings indicated that WT was also an important factor affecting CH<sub>4</sub> concentration. An increase in temperature enhances the CH<sub>4</sub> production capacity by promoting the activity of methanogens and related enzymes (Yvon-Durocher et al., 2014). Furthermore, algal blooms are more likely to occur with increasing temperature (Paerl et al., 2012), which also enhances net CH<sub>4</sub> production and consequently increases the dissolved CH<sub>4</sub> concentration.

#### 4.2. Comparison with other studies

We measured the CH<sub>4</sub> concentrations based on MIMS. The mean CH<sub>4</sub> concentration over five months was  $0.58 \pm 0.65 \mu\text{mol L}^{-1}$ , which was lower than the global mean value ( $1.35 \pm 5.16 \mu\text{mol L}^{-1}$ ) (Stanley et al., 2016). Although the concentration of CH<sub>4</sub> was low compared with the global average, the high CH<sub>4</sub> saturation ratios indicate that gravel-bed urban rivers with very little organic sediment still have strong CH<sub>4</sub> emission potential. The mean CH<sub>4</sub> concentration of this study was much lower than that of the other two urban rivers recently investigated by Zhang et al. (2021b) and Wang et al. (2021) in the Chaohu Lake Basin, China, and Beijing, China, respectively (mean CH<sub>4</sub> concentrations were  $5.5$  and  $2.5 \mu\text{mol L}^{-1}$ , respectively). A possible reason for this is that the riverbed is stony, and there are very few organic sediments in the mainstream Xin'an River. Our incubation experiment showed that the addition of organic solids potentially increased the CH<sub>4</sub> concentration in the water column, which is consistent with several studies that reported that organic sediment was a hotspot of CH<sub>4</sub> production (Conrad et al., 2009; Mach et al., 2015; Emilson et al., 2018), and CH<sub>4</sub> diffusion from organic sediment was an important source of water column CH<sub>4</sub> (Martens et al., 1980). In addition, the eutrophication degree of the Xin'an River was lower than that of the urban rivers mentioned above. According to our results and previous studies, eutrophication can significantly affect CH<sub>4</sub> concentrations in the water column, which may also be a vital reason for the low CH<sub>4</sub> concentration in our study areas.

#### 4.3. Implications for management

Reducing eutrophication is an effective method that can control CH<sub>4</sub>

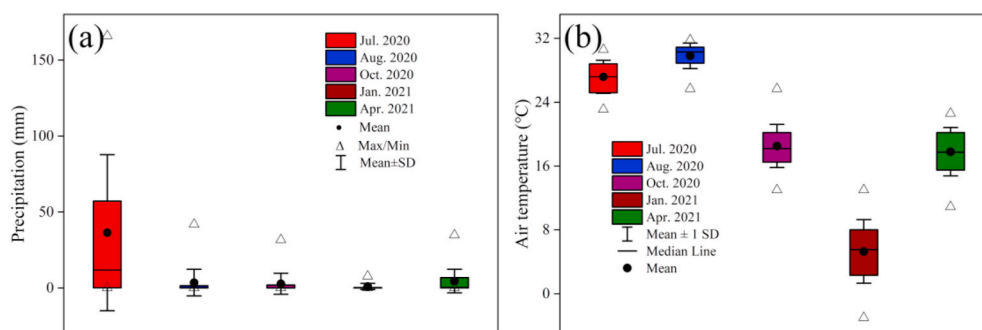


Fig. 7. Precipitation (a) and air temperature (b) in the five sampling months. The bottom line, middle line, and the top line of the box plot indicate the values at 25%, 50%, and 75%, respectively.



production and emission, as reported by numerous studies (Davidson et al., 2018; Beaulieu et al., 2019). However, not only nutrients (mainly nitrogen and phosphorus) but also the N:P ratios should be taken into consideration in the management of CH<sub>4</sub> production because we noticed that the CH<sub>4</sub> saturation ratio was negatively correlated with the N:P ratios (Fig. 4). This negative correlation may have been due to biological nitrogen fixation since the low N:P ratio was beneficial for nitrogen-fixing cyanobacterial growth, which could enhance CH<sub>4</sub> production and increase the CH<sub>4</sub> concentration. As a result, we recommend that nitrogen control should be applied cautiously in nitrogen-limited waters in the management of eutrophication, as well as in CH<sub>4</sub> mitigation.

The positive relationship between the CH<sub>4</sub> saturation ratio and WT (Fig. 4) indicates that the potential for CH<sub>4</sub> production and emission can be enhanced with increasing temperature. The temperature of urban regions is normally 2–4 °C higher than that in nonurban areas due to the heat island effect (Liu et al., 2015). In addition, heatwaves under climate change may also enhance methanogenesis and algal blooms, leading to intense CH<sub>4</sub> production and emission. Overall, the global warming caused by greenhouse gas (CH<sub>4</sub>, N<sub>2</sub>O, CO<sub>2</sub>, etc.) emissions can provide a positive feedback on CH<sub>4</sub> production. Thus, urban wastewater should be treated efficiently to remove nutrients and organic matter. Furthermore, we observed that the CH<sub>4</sub> concentrations were much higher in the sampling sites near the large WWTP (Fig. 3d), indicating that municipal WWTPs should improve sewage treatment efficiency to reduce the CH<sub>4</sub> level in wastewater.

Organic sediment is one of the important sources of nutrients in the water column (Percuoco et al., 2015) and may become an important driving factor for algal growth (Wu et al., 2017). Sediment dredging is considered to be an effective measure to reduce nutrient release from organic sediment (Moore et al., 2017). In the Xin'an River with very little organic sediment, we observed that the concentrations of dissolved CH<sub>4</sub> and nutrients in the water were generally lower than those in some urban rivers with a large amount of organic sediment. Our incubation experiments show that the presence of organic soils can potentially enhance CH<sub>4</sub> production, along with the increase in CH<sub>4</sub> concentration in the water column (Fig. 6a). Moreover, the presence of organic soils can significantly increase the concentration of nutrients in the water and consequently induce the growth of algae (Fig. 6c). Therefore, dredging organic sediment in 'normal' urban rivers (urban rivers with a large amount of organic sediments) that are seriously affected by human activities may be feasible in controlling nutrient release from organic sediment, alleviating algal blooms, and reducing CH<sub>4</sub> concentrations and emissions.

#### 4.4. Limitations of this study

In this study, we only measured the dissolved CH<sub>4</sub> concentrations and calculated the CH<sub>4</sub> saturation ratios. Neither diffusive nor ebullitive fluxes were directly measured. Consequently, we could not accurately quantify the CH<sub>4</sub> emission from oxic urban rivers such as the Xin'an River and compare it with the global mean value. Additionally, CH<sub>4</sub> ebullition was reported to be more important than diffusion in shallow rivers due to the presence of a large amount of organic sediment (Wang et al., 2021). However, the contribution of CH<sub>4</sub> ebullition to total CH<sub>4</sub> emissions in gravel-bed rivers with very little organic sediment, such as the Xin'an River, is still unclear and is an important issue for future research. CH<sub>4</sub> oxidation is a vital pathway that can reduce CH<sub>4</sub> in water bodies (Hao et al., 2020; Xia et al., 2021). However, we did not quantify the CH<sub>4</sub> oxidation capacity in this study. Future studies can focus on CH<sub>4</sub> oxidation in gravel-bed urban rivers such as the Xin'an River and can calculate its contribution to CH<sub>4</sub> reduction. Lastly, although our incubation experiments and field observations suggest that algae can produce CH<sub>4</sub> under oxic conditions and may further affect the CH<sub>4</sub> concentration in the water column, their specific contribution to the total CH<sub>4</sub> concentration in gravel-bed urban rivers with very little

organic sediment is still not clear and is worth studying in the future.

## 5. Conclusions

The Xin'an River is a gravel-bed urban river with very little organic sediment and high DO concentrations. Using a membrane inlet mass spectrometer, we measured the dissolved CH<sub>4</sub> concentrations and calculated the CH<sub>4</sub> saturation ratios for five months, including four seasons and a rainy month. The results showed that CH<sub>4</sub> was supersaturated across all sampling sites in the five months, which suggested that gravel-bed urban rivers with very little organic sediment also have large CH<sub>4</sub> emission potential. The significant correlation between the CH<sub>4</sub> saturation ratio and Chl<sub>a</sub> concentration and evident CH<sub>4</sub> accumulation in the oxic water column during incubation when algae were added indicated that algae may be a potential factor that can affect the CH<sub>4</sub> concentration in oxic waters; however, their specific contribution to the total CH<sub>4</sub> concentration in the water column remains unknown. The water CH<sub>4</sub> concentrations were significantly higher in the downstream river than in the upstream river, indicating that human activities along the river had a large impact on CH<sub>4</sub> concentrations. Other factors, such as WT, heavy rainfall events, and organic matter, can also potentially affect the CH<sub>4</sub> concentration in such rivers. Furthermore, the algal blooms caused by human discharged nutrients can potentially increase the CH<sub>4</sub> levels in river water. Based on our results, necessary measures should be considered to reduce the CH<sub>4</sub> concentrations in urban rivers, such as reducing the concentrations of nutrients, organic matter, and CH<sub>4</sub> in wastewater from human activities.

### Credit author statement

Feng Zhao: Conceptualization; Data curation; Formal analysis; Investigation; Methodology; Software; Visualization; Roles/Writing - original draft. Yongqiang Zhou, Wei Zou and Mengyuan Zhu: Writing - review & editing. Guangwei Zhu: Funding acquisition; Hai Xu: Funding acquisition; Investigation; Project administration; Resources; Supervision; Validation; Writing - review & editing. Xu Zhan, Lijuan Kang and Xingchen Zhao: Investigation.

### Declaration of competing interest

The authors declare that they have no known competing financial interests or personal relationships that could have appeared to influence the work reported in this paper.

### Acknowledgments

This research was supported by the Strategic Priority Research Program of Chinese Academy of Sciences (XDA23040201) and the National Natural Science Foundation of China (41830757, 42077161).

### Appendix A. Supplementary data

Supplementary data to this article can be found online at <https://doi.org/10.1016/j.envpol.2021.118769>.

### References

- Alshboul, Z., Encinas-Fernandez, J., Hofmann, H., Lonke, A., 2016. Export of dissolved methane and carbon dioxide with effluents from municipal wastewater treatment plants. *Environ. Sci. Technol.* 50 (11), 5555–5563.
- Angel, R., Matthies, D., Conrad, R., 2011. Activation of methanogenesis in arid biological soil crusts despite the presence of oxygen. *PLoS One* 6 (5), e20453.
- APHA, 2012. Standard Methods for Examination of Water and Wastewater 22ed. American Public Health Association, Washington.
- Bastviken, D., Tranvik, L.J., Downing, J.A., Crill, P.M., Enrich-Prast, A., 2011. Freshwater methane emissions offset the continental carbon sink. *Science* 331 (6013), 50.

- Batista, A.M.M., Woodhouse, J.N., Grossart, H.P., Giani, A., 2019. Methanogenic archaea associated to *Microcystis* sp. in field samples and in culture. *Hydrobiologia* 831, 163–172.
- Beaulieu, J.J., Jake, J., DelSontro, T., Downing, J.A., 2019. Eutrophication will increase methane emissions from lakes and impoundments during the 21st century. *Nat. Commun.* 10, 1375.
- Berg, A., Lindblad, P., Svensson, B.H., 2014. Cyanobacteria as a source of hydrogen for methane formation. *World J. Microbiol. Biotechnol.* 30 (2), 539–545.
- Bizic, M., Klintzsch, T., Ionescu, D., Hindiyyeh, M.Y., Günthel, M., Muro-Pastor, A.M., Eckert, W., Ulrich, T., Keppler, F., Grossart, H.-P., 2020. Aquatic and terrestrial cyanobacteria produce methane. *Sci. Adv.* 6 (3), eaax5343.
- Borges, A.V., Darchambeau, F., Lambert, T., Bouillon, S., Morana, C., Brouyere, S., Hakoun, V., Jurado, A., Tseung, H.C., Descy, J.P., Roland, F.A., 2018. Effects of agricultural land use on fluvial carbon dioxide, methane and nitrous oxide concentrations in a large European river, the Meuse (Belgium). *Sci. Total Environ.* 610–611, 342–355.
- Clough, T.J., Buckthought, L.E., Kelliher, F.M., Sherlock, R.R., 2007. Diurnal fluctuations of dissolved nitrous oxide ( $N_2O$ ) concentrations and estimates of  $N_2O$  emissions from a spring-fed river: implications for IPCC methodology. *Global Change Biol.* 13 (5), 1016–1027.
- Conrad, R., Seiler, W., 1980. Contribution of hydrogen production by biological nitrogen fixation to the global hydrogen budget. *J. Geophys. Res. Oceans* 85 (C10), 5493–5498.
- Conrad, R., Claus, P., Gasper, P., 2009. Characterization of stable isotope fractionation during methane production in the sediment of a eutrophic lake, Lake Dagow, Germany. *Limnol. Oceanogr.* 54 (2), 457–471.
- Cook, K.V., Li, C., Cai, H., Krumholz, L.R., Hambright, D., Paerl, H.W., Steffen, M.M., Wilson, A.E., Burford, M.A., Grossart, H.P., Hamilton, D.P., Jiang, H., Sukenik, A., Latour, D., Meyer, E.L., Padisák, J., Qin, B., Zamor, R.M., Zhu, G., 2019. The global *Microcystis* interactome. *Limnol. Oceanogr.* 65 (S1), S194–S207.
- Damm, E., Helmke, E., Thoms, S., Schauer, U., Kiene, R.P., 2010. Methane production in aerobic oligotrophic surface water in the central Arctic Ocean. *Biogeosciences* 7 (3), 46–48.
- Davidson, T.A., Audet, J., Jeppesen, E., Landkildehus, F., Lauridsen, T.L., Søndergaard, M., Syvaranta, J., 2018. Synergy between nutrients and warming enhances methane ebullition from experimental lakes. *Nat. Clim. Change* 8 (2), 156.
- de Angelis, M.A., Lee, C., 1994. Methane production during zooplankton grazing on marine phytoplankton. *Limnol. Oceanogr.* 39 (6), 1298–1308.
- Deemer, B.R., Harrison, J.A., Li, S., Beaulieu, J.J., DelSontro, T., Barros, N., Bezerra-Neto, J.F., Powers, S.M., dos Santos, M.A., Vonk, J.A., 2016. Greenhouse gas emissions from reservoir water surfaces: a new global synthesis. *Bioscience* 66 (11), 949–964.
- Donis, D., Flury, S., Stöckli, A., Spangenberg, J.E., Vachon, D., McGinnis, D.F., 2017. Full-scale evaluation of methane production under oxic conditions in a mesotrophic lake. *Nat. Commun.* 8, 1661.
- Emilson, E.J.S., Carson, M.A., Yakimovich, K.M., Osterholz, H., Dittmar, T., Gunn, J.M., Mykityczuk, N.C.S., Basiliko, N., Tanentzap, A.J., 2018. Climate-driven shifts in sediment chemistry enhance methane production in northern lakes. *Nat. Commun.* 9, 1801.
- Günthel, M., Donis, D., Kirillin, G., Lonescu, D., Bizic, M., McGinnis, D.F., Grossart, H., Tang, K.W., 2019. Contribution of oxic methane production to surface methane emission in lakes and its global importance. *Nat. Commun.* 10, 5479.
- Günthel, M., Klawonn, I., Woodhouse, J., Bizic, M., Ionescu, D., Ganzert, L., Kümmel, S., Nijenhuis, L., Zoccarato, L., Grossart, H., Tang, K.M., 2020. Photosynthesis-driven methane production in oxic lake water as an important contributor to methane emission. *Limnol. Oceanogr.* 65 (12), 2853–2865.
- Hao, Q., Liu, F., Zhang, Y., Wang, O., Xiao, L., 2020. *Methylobacter* accounts for strong aerobic methane oxidation in the Yellow River Delta with characteristics of a methane sink during the dry season. *Sci. Total Environ.* 704, 135383.
- Hlaváčová, E., Rulík, M., Čáp, L., 2005. Anaerobic microbial metabolism in hyporheic sediments of a gravel bar in a small lowland stream (Sitka stream, Czech Republic). *River Res. Appl.* 21 (9), 1003–1011.
- Hofmann, H., Federwisch, L., Peeters, F., 2010. Wave-induced release of methane: littoral zones as a source of methane in lakes. *Limnol. Oceanogr.* 55 (5), 1990–2000.
- Hu, H.J., Wei, Y.X., 2007. *The Freshwater Algae of China: Systematics, Taxonomy and Ecology*. Science Press, Beijing.
- IPCC, 2013. *Climate Change 2013: the Physical Science Basis. Contribution of Working Group I to the Fifth Assessment Report of the Intergovernmental Panel on Climate Change*. United Nations, Geneva.
- Kana, T.M., Darkangelo, C., Hunt, M.D., Oldham, J.B., Bennett, G.E., Cornwell, J.C., 1994. Membrane inlet mass spectrometer for rapid high-precision determination of  $N_2$ ,  $O_2$ , and Ar in environmental water samples. *Anal. Chem.* 66 (23), 4166–4170.
- Karl, D.M., Beversdorf, L., Björkman, K.M., Church, M.J., Martinez, A., Delong, E.F., 2008. Aerobic production of methane in the sea. *Nat. Geosci.* 1, 473–478.
- Li, X., Yao, H., Yu, Y., Cao, Y., Tang, C., 2020. Greenhouse gases in an urban river: trend, isotopic evidence for underlying processes, and the impact of in-river structures. *J. Hydrol.* 591, 125290.
- Liu, K., Chen, S., Zhang, L., Yang, H., Zhang, R., Li, X., 2015. Analysis of the urban heat island effect in Shijiazhuang, China using satellite and airborne data. *Rem. Sens.* 7, 4804–4833.
- Loeks-Johnson, B.M., Cotner, J.B., 2020. Upper Midwest lakes are supersaturated with  $N_2$ . *Proc. Natl. Acad. Sci. U. S. A.* 117 (29), 17063–17067.
- Mach, V., Blaser, M.B., Claus, P., Chaudhary, P.P., Rulík, M., 2015. Methane production potentials, pathways, and communities of methanogens in vertical sediment profiles of river Sitka. *Front. Microbiol.* 6 (506).
- Martens, C.S., Klump, J.V., 1980. Biogeochemical cycling in an organic-rich coastal marine basin—I. Methane sediment-water exchange processes. *Geochem. Cosmochim. Acta* 44 (3), 471–490.
- McGinnis, D.F., Bilsley, N., Schmidt, M., Fietzke, P., Bodmer, P., Premke, K., Lorke, A., Flury, S., 2016. Deconstructing methane emissions from a small Northern European river: hydrodynamics and temperature as key drivers. *Environ. Sci. Technol.* 50 (21), 11680–11687.
- Montzka, S.A., Dlugokencky, E.J., Butler, J.H., 2011. Non- $CO_2$  greenhouse gases and climate change. *Nature* 476, 43–50.
- Moore, M., Locke, M.A., Jenkins, M., Steinriede, R.W., McChesney, D.S., 2017. Dredging effects on selected nutrient concentrations and ecoczymatic activity in two drainage ditch sediments in the lower Mississippi River Valley. *Int. Soil Water Conserv. Res.* 5 (3), 190–195.
- Ortega, S.H., González-Quijano, C.R., Casper, P., Singer, G.A., Gessner, M.O., 2019. Methane emissions from contrasting urban freshwaters: rates, drivers, and a whole-city footprint. *Global Change Biol.* 25 (12), 4234–4243.
- Paerl, H.W., Paul, V.J., 2012. Climate change: links to global expansion of harmful cyanobacteria. *Water Res.* 46 (5), 1349–1363.
- Percuoco, V.P., Kalnejais, L.H., Officer, L.V., 2015. Nutrient release from the sediments of the great bay estuary, N.H. USA. *Estuarine. Coast. Shelf Sci.* 161, 76–87.
- Reynolds, C.S., 2006. *Ecology of Phytoplankton*. Cambridge University Press, Cambridge.
- Schmale, O., Karle, M., Glockzin, M., Schneider, B., 2019. Potential of nitrogen/argon analysis in surface waters in the examination of areal nitrogen deficits caused by nitrogen fixation. *Environ. Sci. Technol.* 53 (12), 6869–6876.
- Shi, W., Du, M., Ye, C., Zhang, Q., 2021. Divergent effects of hydrological alteration and nutrient addition on greenhouse gas emissions in the water level fluctuation zone of the Three Gorges Reservoir, China. *Water Res.* 201, 117308.
- Smith, V.H., 1983. Low nitrogen to phosphorus ratios favor dominance by blue green algae in lake phytoplankton. *Science* 221, 669–671.
- Stanley, E.H., Casson, N.J., Christel, S.T., Crawford, J.T., Loken, L.C., Oliver, S.K., 2016. The ecology of methane in streams and rivers: patterns, controls, and global significance. *Ecol. Monogr.* 86 (2), 146–171.
- Sun, Q.-Q., Shi, K., Damerell, P., Whitham, C., Yu, G.-H., Zou, C.-L., 2013. Carbon dioxide and methane fluxes: seasonal dynamics from inland riparian ecosystems, northeast China. *Sci. Total Environ.* 465, 48–55.
- Tang, K.W., McGinnis, D.F., Frindte, K., Brüchert, V., Grossart, H.P., 2014. Paradox reconsidered: methane oversaturation in well-oxygenated lake waters. *Limnol. Oceanogr.* 59, 275–284.
- Tang, K.W., McGinnis, D.F., Ionescu, D., Grossart, H., 2016. Methane production in oxic lake waters potentially increases aquatic methane flux to air. *Environ. Sci. Technol. Lett.* 3 (6), 227–233.
- Taylor, K.A., Risk, D., Williams, J.P., Wach, G.D., Sherwood, O.A., 2021. Occurrence and origin of groundwater methane in the stellarton basin, Nova Scotia, Canada. *Sci. Total Environ.* 754, 141888.
- Wang, J., Zhang, J., Xie, H., Qi, P., Ren, Y., Hu, Z., 2011. Methane emissions from a full-scale A/A/O wastewater treatment plant. *Bioresour. Technol.* 102 (9), 5479–5485.
- Wang, R., Zhang, H., Zhang, W., Zheng, X., Butterbach-Bahl, K., Li, S., Han, S., 2020a. An urban polluted river as a significant hotspot for water-atmosphere exchange of  $CH_4$  and  $N_2O$ . *Environ. Pollut.* 264, 114770.
- Wang, Y., Levis, J.W., Barlaz, M.A., 2020b. An assessment of the dynamic global warming impact associated with long-term emissions from landfills. *Environ. Sci. Technol.* 54 (3), 1304–1313.
- Wang, G., Xia, X., Liu, S., Zhang, L., Zhang, S., Wang, J., Xi, N., Zhang, Q., 2021. Intense methane ebullition from urban inland waters and its significant contribution to greenhouse gas emissions. *Water Res.* 189, 116654.
- White, A.E., Karl, D.M., Björkman, K.M., Beversdorf, L.J., Letelier, R.M., 2010. Phosphonate metabolism by *Trichodesmium* IMS101 and the production of greenhouse gases. *Limnol. Oceanogr.* 55 (4), 1755–1767.
- Wu, Z., Liu, Y., Liang, Z., Wu, S., Guo, H., 2017. Internal cycling, not external loading, decides the nutrient limitation in eutrophic lake: a dynamic model with temporal Bayesian hierarchical inference. *Water Res.* 116, 231–240.
- Xia, F., Jiang, Q., Zhu Zou, B., Liu, H., Quan, Z., 2021. Ammonium promoting methane oxidation by stimulating the Type Ia methane-oxidizing bacteria in tidal flat sediments of the Yangtze River estuary. *Sci. Total Environ.* 793, 148470.
- Xiao, Q., Zhang, M., Hu, Z., Gao, Y., Hu, C., Liu, C., Liu, S., Zhang, Z., Zhao, J., Xiao, W., Lee, X., 2017. Spatial variations of methane emission in a large shallow eutrophic lake in sub-tropical climate. *J. Geophys. Res. Biogeosci.* 122 (7), 1597–1614.
- Xiao, Q., Hu, Z., Hu, C., Islam, A.R.M.T., Bian, H., Chen, S., Liu, C., Lee, X., 2021. A highly agricultural river network in Jurong Reservoir watershed as significant  $CO_2$  and  $CH_4$  sources. *Sci. Total Environ.* 769, 144558.
- Yin, H., Islam, M.S., Ju, M., 2021. Urban river pollution in the densely populated city of Dhaka, Bangladesh: big picture and rehabilitation experience from other developing countries. *J. Clean. Prod.* 321, 129040.
- Yvon-Durocher, G., Allen, A.P., Bastviken, D., Conrad, R., Gudas, C., St-Pierre, A., Thanh-Duc, N., del Giorgio, P.A., 2014. Methane fluxes show consistent temperature dependence across microbial to ecosystem scales. *Nature* 507 (7493), 488–491.
- Zamanpour, M.K., Kaliappan, R.S., Rockne, K.J., 2020. Gas ebullition from petroleum hydrocarbons in aquatic sediments: a review. *J. Environ. Manag.* 271, 110997.
- Zhang, L., Liao, Q., Gao, R., Luo, R., Liu, C., Zhong, J., Wang, Z., 2021a. Spatial variations in diffusive methane fluxes and the role of eutrophication in a subtropical shallow lake. *Sci. Total Environ.* 759, 143495.
- Zhang, W., Li, H., Xiao, Q., Li, X., 2021b. Urban rivers are hotspots of riverine greenhouse gas ( $N_2O$ ,  $CH_4$ ,  $CO_2$ ) emissions in the mixed-landscape Chaohu Lake Basin. *Water Res.* 189, 116624.

- Zhao, F., Xu, H., Kana, T., Zhu, G., Zhan, X., Zou, W., Zhu, M., Kang, L., Zhao, X., 2021. Improved membrane inlet mass spectrometer method for measuring dissolved methane concentration and methane production rate in a large shallow lake. *Water* 13 (19), 2699.
- Zhao, F., Zhan, X., Xu, H., Zhu, G., Zou, W., Zhu, M., Kang, L., Guo, Y., Zhao, X., Wang, Z., Tang, W., 2022. New insights into eutrophication management: importance of temperature and water residence time. *J. Environ. Sci.* 111, 229–239.
- Zheng, Y., Harris, D.F., Yu, Z., Fu, Y., Poudel, S., Ledbetter, R.N., Fixen, K.R., Yang, Z., Boyd, E.S., Lidstrom, M.E., Seefeldt, L.C., Harwood, C.S., 2018. A pathway for biological methane production using bacterial iron-only nitrogenase. *Nat. Microbiol.* 3, 281–286.
- Zou, W., Zhu, G., Cai, Y., Xu, H., Zhu, M., Gong, Z., Zhang, Y., Qin, B., 2020. Quantifying the dependence of cyanobacterial growth to nutrient for the eutrophication management of temperate-subtropical shallow lakes. *Water Res.* 177, 115806.